Delays in dwarf novae I: The case of SS Cygni

M. R. Schreiber, J. -M. Hameury, J. -P. Lasota

A&A 410, 239–252 (2003)
DOI: 10.1051/0004-6361:20031221

Astronomy & Astrophysics

Delays in dwarf novae I: The case of SS Cygni

M. R. Schreiber[1], J.-M. Hameury[1], and J.-P. Lasota[2]

[1] UMR 7550 du CNRS, Observatoire de Strasbourg, 11 rue de l'Université, 67000 Strasbourg, France
e-mail: hameury@astro.u-strasbg.fr
[2] Institut d'Astrophysique de Paris, 98bis boulevard Arago, 75014 Paris, France
e-mail: lasota@iap.fr

Received 27 May 2003 / Accepted 25 July 2003

Abstract. Using the disc instability model and a simple but physically reasonable model for the X-ray, extreme UV, UV and optical emission of dwarf novae we investigate the time lags observed between the rise to outburst at different wavelengths. We find that for "normal", i.e. fast-rise outbursts, there is good agreement between the model and observations provided that the disc is truncated at a few white dwarf radii in quiescence, and that the viscosity parameter α is ∼0.02 in quiescence and ∼0.1 in outburst. In particular, the increased X-ray flux between the optical and EUV rise and at the end of an outburst, is a natural outcome of the model. We cannot explain, however, the EUV delay observed in anomalous outbursts because the disc instability model in its standard α-prescription form is unable to produce such outbursts. We also find that the UV delay is, contrary to common belief, slightly longer for inside-out than for outside-in outbursts, and that it is not a good indicator of the outburst type.

Key words. accretion, accretion discs – instabilities – stars: individual: SS Cygni – stars: novae, cataclysmic variables – stars: binaries : close

1. Introduction

Dwarf novae are cataclysmic variables (CVs) in which the accretion disc is subject to a thermal-viscous instability resulting in recurrent outbursts lasting for a few days and separated by weeks (see Warner 1995 for an encyclopedic review of CVs and Lasota 2001 for a recent review of the disc instability model). Their study has received considerable attention, since these systems are often bright, usually vary on short time scales and are relatively easy to observe so they are an excellent testing ground for the mechanisms transporting angular momentum in accretion discs which, despite very significant recent progress, are not yet fully understood (see Balbus & Hawley 1998; Balbus 2002, for recent reviews).

The disc instability model (DIM) is based on the existence of a thermal-viscous instability in regions where hydrogen is partially ionized, and opacities depend strongly on temperature. If one plots a disc's thermal equilibria as the effective disc temperature $T_{\rm eff}$ at a given radius r (or equivalently for viscous equilibria the mass transfer rate $\dot{M}$) as a function of the disc surface density Σ, one obtains the well known S-curve, in which the upper (hot) and lower (cold) branches are stable and the intermediate one is unstable. These branches are delimited by two critical values of Σ, $\Sigma_{\rm max}$ above which no cool solution exists, and $\Sigma_{\rm min}$ below which no hot solution is possible.

Send offprint requests to: M. R. Schreiber,
e-mail: mschrei@astro.u-strasbg.fr

Provided that the mass transfer rate from the secondary corresponds somewhere in the disc to this unstable branch, the disc will not be steady. In quiescence, matter is accreted onto the white dwarf at a rate lower than the rate at which it is transferred from the secondary; the disc stays on the lower branch of the S-curve. The disc mass therefore grows, and, at some point, Σ reaches $\Sigma_{\rm max}$; the temperature increases locally, and a heating fronts forms that propagate towards the white dwarf and towards the outer disc edge. Matter then accretes faster than transferred from the white dwarf, the disc empties, and a cooling front eventually starts from the outer edge of the disc that brings the system into quiescence.

If the mass transfer rate is high, the accumulation time at the outer disc edge can be shorter than the viscous diffusion time, and the instability will be triggered in the disc outer regions; the outburst is of the outside-in type. On the other hand, for low mass transfer rates, the viscous time is the shortest, and the outburst will be triggered at the inner edge; the outburst is of the inside-out type. The limit between both types of outburst therefore depends sensitively on parameters such as the mass transfer rate, and the viscosity; it is therefore important to be able to determine the type of observed outbursts for constraining these parameters. Models predict that the outburst light curve is asymmetric in the outside-in case, with a sharp rise and a longer decay, whereas the rise and decay time should be of the same order in the inside-out case. It is however not an easy task to guess the outside-in nature of an outburst from its

light curve: models sometimes produce asymmetric outbursts which are of the inside-out type (Buat-Ménard et al. 2001).

Another difference that has often been put forward to distinguish both types of outburst is the existence of a delay between the UV and the optical rise during an outburst, the so-called UV delay which has been measured for several dwarf novae. As UV radiation is emitted close to the white dwarf, one would naively expect that there should be a long delay in cases where the outburst is triggered in the disc outer regions, and no delay when the outburst starts at the inner disc edge.

Recently, time lags similar to the UV delay have been observed between the optical rise, an increase of X-ray emission and the EUV light curve (Mauche et al. 2001; Wheatley et al. 2003). Especially the long orbital period, very bright dwarf nova SS Cygni has intensively been monitored simultaneously at different wavelengths. For four outbursts the EUV delay has been measured and SS Cyg is the only dwarf nova system for which the evolution of the X-ray emission throughout an outburst is available. As in the case of the UV delay, differences in the observed EUV delay have been interpreted as an indicator for the outburst type (Mauche et al. 2001; Cannizzo 2001).

There has been a long debate about the ability of the DIM to reproduced observed UV delays. Smak (1998) showed that the asserted inability of the DIM to reproduce delays results from the inadequacy of the numerical scheme used. The outburst type, and hence the resulting delays, depend strongly on the modeling itself; in particular, it is very difficult to obtain outbursts of the outside-in type when the outer disc edge is kept fixed to a given value (Hameury et al. 1998). Similarly, the heating of the outer regions by effects such as the impact of the stream of matter flowing from the secondary, or tidal torques dissipation also influences the nature of the outbursts.

In this paper, contrary to the previous studies of the UV and other delays, we use a version of the DIM (Buat-Ménard et al. 2001) which allows describing of the SS Cyg outburst cycle with the real parameters (especially the large disc size and mass-transfer rates corresponding to outside-in outbursts) of this system. We use simple but reasonable assumptions about the emission from the boundary layer to investigate multi–wavelengths observations of this observationally best studied dwarf nova. The paper is organized as follows. Having reviewed the observations in Sect. 2 we present our model in Sect. 3 and its predictions for SS Cygni in Sect. 4. Finally we compare our results with those of previous studies (Sect. 5) and discuss them in the light of the observations (Sect. 6).

2. Reviewing the observations

SS Cygni has become the classical dwarf nova system for analyzing the mechanism of dwarf nova outbursts because a detailed visual long term light curve of rather regular outburst behaviour is available (see Fig. 1 for snapshots of the light curve and Cannizzo & Mattei 1992 for a detailed light curve analysis). In addition, SS Cyg has been intensively observed at shorter wavelengths:

(1) In quiescence as well as during outburst SS Cyg is – as dwarf novae in general – a source of X-ray emission. Spectral fits to the X-ray flux observed in quiescence suggest a Bremsstrahlung origin from gas with temperatures of 2−20 keV and luminosities of the order of a few $10^{32}\,d_{100}^2\,\mathrm{erg\,s^{-1}}$ where d_{100} is the distance in units of 100 pc (Yoshida et al. 1992; Done & Osborne 1997; Ponman et al. 1995). Relating this X-ray luminosity to the emission from the boundary layer requires an accretion rate of $\dot{M}_{\rm acc} \sim 10^{15}\,d_{100}^2\,\mathrm{g\,s^{-1}}$, assuming gravitational energy conversion onto a 1.0 $M_\odot$white dwarf.

(2) Cannizzo et al. (1986) present simultaneous observations in the UV and optical during an outburst and find the rise of the UV flux being delayed to the optical by ∼0.5 days ($\Delta_{\rm UV,0}$ and $\Delta_{\rm UV,0.5}$ in Table 1).

(3) Further simultaneous observations of SS Cyg at optical and EUV wavelengths have been published for four outbursts of SS Cygni (Mauche et al. 2001). Two of these outbursts are called "normal" outbursts (marked with "n" in Fig. 1 and Table 1) which refers to the observed fast optical rise. The time lag between the optical and the EUV is $\Delta_{\rm EUV,0} \approx \Delta_{\rm EUV,0.5} \sim 1.5$ days for these outbursts, i.e. the EUV delay is almost independent on where one measures the delay. In contrast, the EUV delay measured for the two "anomalous" outbursts (i.e. outbursts with a slow optical rise, denoted with a in Fig. 1 and Table 1) is essentially longer at the onset of the optical rise

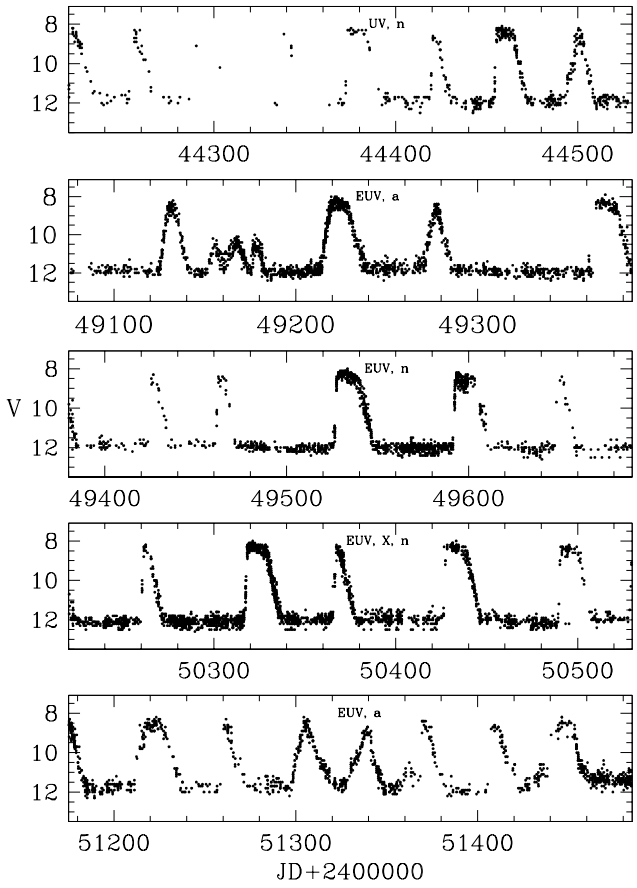

Fig. 1. Snapshots of the visual light curve of SS Cyg. The five panels show parts of the light curve including the outbursts for which observations in the UV, EUV, or X-ray range exist (see Table 1). Outbursts called normal (anomalous) are marked with "n" ("a"). The data is taken from the AFOEV.

Table 1. Outbursts of SS Cyg observed at different wavelengths and the resulting delays. The quantities X_{on} (X_{off}) denote the time lag measured between the optical rise and the increase (decrease) of the X-ray emission. The UV and EUV delays are measured at the beginning of the optical rise (index 0) and at the half the maximum optical flux (index 0.5) where also the width (W) of the outbursts is measured. Outbursts with a slow optical rise are called "anomalous" (type "a") whereas the optical flux increases rapidly in the case of "normal" outbursts (type "n").

Instrument	JD+2 440 000	X_{on} [d]	X_{off} [d]	$\Delta_{EUV,0}$ [d]	$\Delta_{EUV,0.5}$ [d]	$\Delta_{UV,0}$ [d]	$\Delta_{UV,0.5}$ [d]	W [d]	Type	Ref.
Voyager	4372	–	–	–	–	∼0.5	∼0.5	15	n	(1)
EUVE	9220	–	–	3.0	∼0.0	–	–	17	a	(2)
EUVE	9530	–	–	1.5	∼1.5	–	–	15	n	(2)
EUVE & RXTE	10370	0.9	1.4	1.5	∼1.5	–	–	8	n	(2), (3), (4)
EUVE	11335	–	–	>5	≳0.5	–	–	8	a	(2)

References: (1) Cannizzo et al. (1986), (2) Mauche et al. (2001), (3) Wheatley (2000), (4) Wheatley et al. (2003).

but decreasing with increasing visual brightness (see $\Delta_{EUV,0}$ and $\Delta_{EUV,0.5}$ in Table 1).
(4) Wheatley (2000) and Wheatley et al. (2003) present simultaneous observations at optical, X-ray, and EUV wavelengths and finds: the hard X-ray flux increases 0.9 d (X_{on} in Table 1) after the optical and half a day before the EUV rise, at which point X-rays are abruptly shut off. X_{off} in Table 1 denotes the time lag between the optical rise and the sudden decrease of X-ray emission. At the end of the optical decline the X-ray emission rises again for approximately two days.

Snapshots of the optical light curve corresponding to the five outbursts for which simultaneous multi–wavelength observations exist (Table 1) are shown in Fig. 1.

3. The model

We use here the version of the DIM described in Hameury et al. (1998) in which heating of the disc by the tidal torque and the stream impact have been incorporated (Buat-Ménard et al. 2001). We detail below the contribution of each constituent of the system to the light curve at various wavelengths; as we shall see, the optical light curve is dominated by the accretion disc, with some contribution from the hot spot and the secondary star; the UV in outburst originates from the disc, and the boundary layer is the source of hard radiation.

3.1. Contribution of the boundary layer

The transition region between the accretion disc and the white dwarf, the boundary layer is generally thought to be a source of UV, EUV and hard X-ray photons. Approximately one half of the accretion energy should be released in this region.

Although the detailed nature of this region is very uncertain, simple models (Pringle & Savonije 1979; Tylenda 1981; Patterson & Raymond 1985b) as well as more detailed calculations (Narayan & Popham 1993) suggest the transition from an optically thin X-ray emitting region to an optically thick boundary layer when the rate at which mass is supplied to the boundary layer from the accretion disc exceeds a certain value around 10^{16} g s^{-1}. Hence, for high accretion rates the optically thick boundary layer is expected to dominate the EUV and soft X-ray emission of dwarf novae whereas for low accretion rates the emission of X-rays is expected.

This picture is not only favoured by pure theoretical arguments but it appears also reasonable considering the observations reviewed in the previous section. We therefore assume here that the boundary layer is optically thin if the mass accretion rate is below $\dot{M}_{cr} = 10^{16}$ g s^{-1} and optically thick otherwise. We assume that the optically thin boundary layer emits hard X-rays proportional to the accretion rate below $\dot{M}_{cr}$:

$$L_X = L_{BL} = \frac{G\dot{M}_{acc}M_{wd}}{2R_{wd}}. \quad (1)$$

The optically thick boundary layer is approximated with a blackbody of the effective temperature

$$T_{BL}^4 = \frac{L_{BL}}{f_{em}\sigma\, 4\pi\, {R_{wd}}^2} = \frac{G\dot{M}_{acc}M_{wd}}{f_{em}\sigma\, 4\pi\, {R_{wd}}^2\, 2R_{wd}}, \quad (2)$$

where f_{em} is a parameter representing the fractional emitting region of the boundary layer. Clearly, the boundary layer will expand with increasing accretion rate, i.e. f_{em} increases with $\dot{M}_{acc}$. We approximate the expansion of the boundary layer with $\dot{M}_{acc}$ following Patterson & Raymond (1985a):

$$f_{em} = 10^{-3}\left(\frac{\dot{M}_{acc}}{10^{16}\mathrm{g s^{-1}}}\right)^{0.28}. \quad (3)$$

with $\dot{M}_{acc,16} = \dot{M}_{acc}/10^{16}$ g s^{-1}.

We are aware of the approximative nature of the above prescription as the choice of $\dot{M}_{cr}$ is somewhat arbitrary and we do not take into account the time it may take the boundary layer to switch between the optically thin and optically thick state. However, observations (see point 4 in the previous section) indicate that the transition is rather immediate and for the purpose of this paper our simple approach is sufficient.

3.2. Thermal emission from the white dwarf

The white dwarf contributes to the total emission, both in the UV and optical. Throughout this paper we assume that the effective temperature of the white dwarf is $T_{wd} = 18\,000$ K. We neglect white dwarf cooling and assume that T_{wd} remains constant; this is justified as long as one is interested only in the initial phases of the outburst (in systems in which white dwarf cooling has been observed, the cooling time is larger than 10 days, Sion 1999). In view of the uncertainties associated with the treatment of the boundary layer, it is sufficient to assume that the spectrum is that of a blackbody.

Table 2. Binary parameter of SS Cyg.

$P_{\rm orb}$/hr	6.6
$M_{\rm wd}/M_\odot$	1.19
$M_{\rm sec}/M_\odot$	0.70
$< R_{\rm out} > /10^{10}$ cm	5.4
$R_{\rm wd}/10^8$ cm	3.9

3.3. The secondary star

In the following (except when otherwise stated) we consider that the secondary is a 0.7 $M_\odot$ main sequence star, with effective temperature 4000 K. The spectrum is taken from Kurucz (1993). During an outburst, the effective temperature of the irradiated hemisphere of the secondary increases, and the spectrum of the secondary becomes the sum of two blackbodies with different effective temperatures, but the same emitting area, provided the luminosity is averaged over the orbital period. We assume here that:

$$T_2^4 = T_*^4 + \left(\frac{R_{\rm wd}}{a}\right)^2 \left\{T_{\rm BL}^4 f_{\rm em} + {T_{\rm wd}}^4\right\} \quad (4)$$

where T_2 and T_* are the effective temperatures of the illuminated and unilluminated hemispheres respectively, $T_{\rm BL}$ is given by Eq. (2), and a is the orbital separation. Note that the disc luminosity does not enter in Eq. (4), because its luminosity is emitted perpendicular to the orbital plane, and only a small fraction of it can effectively heat the secondary.

3.4. The hot spot

In our model, a fraction of the energy released by the impact of the stream onto the disc is assumed to be thermalized, and is already included in the disc model. The remaining fraction is released in the hot spot, for which we assume a blackbody spectrum with an effective temperature of 10 000 K. In the following we assume that one half of the stream impact energy is emitted by the hot spot.

3.5. Disc emission

The local spectrum of the disc is assumed to be given by Kurucz (1979, 1993). This assumption is probably not very good, especially during quiescence, when the optical depth of the disc is not large. Both the spectra observed during quiescence in e.g. HT Cas (Vrielmann et al. 2002) and the predicted ones (Idan et al. 1999) differ from the simple stellar spectra. For comparison, and also to get some hint on the uncertainty linked to the precise modeling of the spectrum, we also calculate the disc spectrum by summing blackbodies.

4. Results

In this section we present the results we obtain applying the model to a system with the orbital parameter of SS Cyg given in Table 2. The mean outer radius $< R_{\rm out} >$ is taken to be the average of r_1, r_2, and $r_{\rm max}$ calculated in Table 1 of Paczynski (1977).

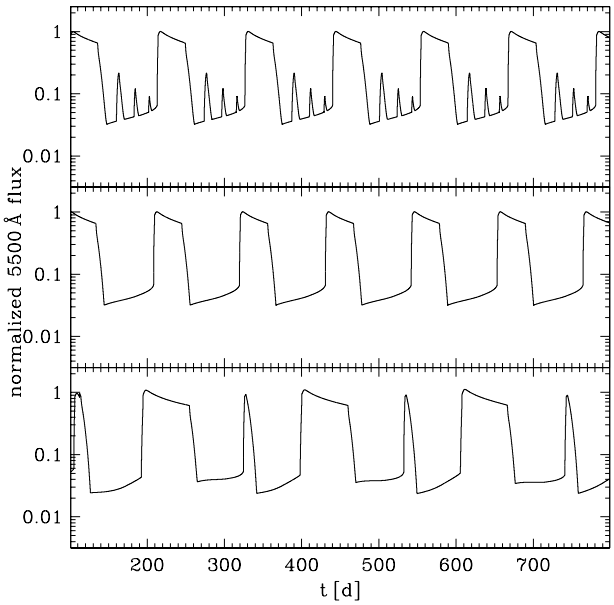

Fig. 2. Calculated long term light curves. From top to bottom: without truncation (model 5), with truncation (model 8), and finally with truncation and assuming that the mass transfer rate varies slightly and smoothly (model 11).

We calculated monochromatic light curves at three wavelengths (λ = (100, 1250, 5500) Å) representative for the EUV, UV, and optical flux. For low accretion rates we additionally assumed the energy released in the boundary layer being related to X-ray emission. In Table 3 we have collected the results of our comprehensive numerical investigation. In particular we studied the influence of three so far rather unconstrained ingredients of the model, i.e. the inner boundary condition, the viscosity parameter α, and the mass transfer rate from the secondary.

In general, the obtained UV emission is rising after the optical flux but before the EUV increases. We find that the delays depend strongly on where we measure them. In Table 3 we therefore give values for time lags at the onset of the optical rise (index 0) and at half the maximum optical emission (index 0.5).

4.1. Fixed inner boundary

Assuming that the disc extends down to the surface of the white dwarf, i.e. $R_{\rm in} = 3.9\times 10^8$ we performed calculations assuming five different mass transfer rates (models 1–5 in Table 3). As in earlier calculations (e.g. Hameury et al. 1998) we find in this case the calculated light curve cycles consisting of several short low amplitude outbursts followed by a larger one (see Fig. 2). This form of the DIM cannot reproduce the observed light-curve of SS Cyg and similar dwarf novae but it can be used to study various density and temperature distributions in the pre-outburst disc. The delays listed in Table 3 refer to the long outbursts.

As expected, the width of these outbursts increases with the mass transfer rate. For high mass transfer rates the

Table 3. Parameter and delays of calculated outbursts. The obtained delays depend on where one measures them; for the UV and EUV we give values at the beginning of the optical rise (index 0) and at half the maximum optical emission (index 0.5) where also the width of the outbursts (W) has been measured. $R_{\rm init}$ denotes the radius where the heating front started. $X_{\rm on}$ is the time lag between the optical rise and increased X-ray emission. The time $X_{\rm off}$ after the optical rise the boundary layer becomes optically thick and the expected X-rays are shut off.

Model	$\dot{M}_{\rm tr}$ [10^{16} g s^{-1}]	$\alpha_{\rm h}$	$\alpha_{\rm c}$	μ_{30}	$X_{\rm on}$ [d]	$X_{\rm off}$ [d]	$\Delta_{\rm EUV,0}$ [d]	$\Delta_{\rm EUV,0.5}$ [d]	$\Delta_{\rm UV,0}$ [d]	$\Delta_{\rm UV,0.5}$ [d]	$R_{\rm init}$ [10^{10} cm]	W [d]
1	8.5	0.1	0.02	0	0.3	0.9	1.0	1.4	0.3	0.8	0.85	7
2	10	0.1	0.02	0	0	1.5	1.6	1.4	1.0	0.7	0.06	14
3	12.5	0.1	0.02	0	0	2.4	2.6	1.5	1.8	1.0	0.06	23
4	13.75	0.1	0.02	0	0.4	1.0	1.1	1.5	0.4	0.9	1.26	25
5	15	0.1	0.02	0	0.45	1.0	1.2	1.5	0.4	0.9	1.35	36
6	11	0.1	0.02	2	0	0.8	0.8	1.6	0.7	1.0	0.25	16
7	13.75	0.1	0.02	2	0	0.8	1.2	1.5	0.8	0.9	0.25	24
8	15	0.1	0.02	2	0.3	0.7	0.9	1.4	0.3	0.7	1.2	37
9	15	0.2	0.02	2	0.2	0.4	0.5	0.6	0.1	0.2	1.40	20
10	15	0.1	0.01	2	0.3	0.7	0.8	1.0	0.1	0.3	1.31	29
11	14.1*	0.1	0.02	2	0	0.8	0.8	1.4	0.8	1.0	0.25	9
	14.1*	0.1	0.02	2	0	0.8	0.8	1.4	0.8	0.9	0.25	60
	14.1*	0.1	0.02	2	0.3	0.7	0.8	1.3	0.3	0.7	1.28	6
	14.1*	0.1	0.02	2	0.3	0.7	0.8	1.2	0.3	0.7	1.32	51

* Variable mass transfer rate (±15%, see text).

accumulation time scale becomes shorter than the viscous diffusion time scale leading to outbursts of the outside–in type; conversely, inside-out outbursts are expected at low mass transfer rates. An exception from this rule is model 1, i.e. the calculation with the lowest mass transfer rate. This happens because the wide outburst is preceded by a large number of low-amplitude inside-out outbursts during which the heating front dies out before reaching the outer regions allowing mass to accumulate there. Figure 3 shows the normalized flux densities at the relevant wavelengths and the heating front velocities for two calculations (models 1, 3) with the disc extending down to the white dwarf.

4.1.1. Inside-out outbursts

At first we consider the properties of *inside–out* outbursts (models 2, 3; left panels of Fig. 3): The optical rise begins immediately when the heating front starts even though this happens close to the white dwarf. With the heating front reaching the outer regions of the disc, the optical rise gets faster and reaches its maximum value when the outer edge of the disc becomes hot and the disc is expanding radially. At large radii the velocity of the heating front increases due to the effects of additional heating of the outer edge (Fig. 3). The UV emission increases immediately after the ignition of the inside–out heating front but the accretion rate in the inner regions of the disc remains rather low. Hence, UV does not even reach one percent of its maximum value during the early stages of the optical rise. The situation is similar but even more drastic for the EUV emission. The mass accretion rate onto the white dwarf stays far below $\dot{M}_{\rm cr}$ until the heating front has reached the outer disc regions. This explains the long delays at the onset of the optical rise i.e. $\Delta_{\rm UV,0}$ and $\Delta_{\rm EUV,0}$. When the heating front has reached more massive outer disc regions, the UV and the EUV emission are rising faster, leading to somewhat decreased delays $\Delta_{\rm UV,0.5}$ and $\Delta_{\rm EUV,0.5}$. Neither the UV nor the EUV reach their maximum value before the disc has adjusted to the quasi stationary outburst state. Concerning the X-ray emission our calculations predict that the emission from the optically thin boundary layer rises immediately when the inside–out heating front is triggered. The slow increase of the mass accretion rate is displayed by the relatively long lasting X-ray emission during the early rise of the outburst (dotted line in the left panel of Fig. 3).

4.1.2. Outside-in outbursts

The overall situation is very different for *outside–in* outbursts where the heating front ignites far away from the white dwarf (models 1, 4 and 5). One should stress here that while inside-out outbursts always start close to the inner disc edge, the outside-in outbursts may start relatively far from the outer rim; as a result two heating fronts propagate and such outbursts are not really purely "outside-in" (see Buat-Ménard et al. 2001, for examples and discussion).

When the front reaches much earlier the outer parts of the disc the optical flux increases sharply immediately after the instability has been triggered. In addition the entire optical rise is shorter as there are two heating fronts in the disc; the outside–in heating front is indeed the fastest one, but both fronts are faster than a pure inside–out heating front (see the bottom panels of Fig. 3). Naively one could expect the UV and EUV delays to be longer than for inside-out outbursts because of this fast optical rise and because the heating front has to reach the inner disc before the UV and EUV fluxes significantly rise. However, the opposite is true. In addition to differences in their propagation direction, outside–in and inside–out fronts differ in many other respects. Inside-out heating fronts must propagate "uphill" against the surface-density and angular-momentum gradients. This makes the propagation difficult and such fronts can be subject to dying before reaching the outer disc

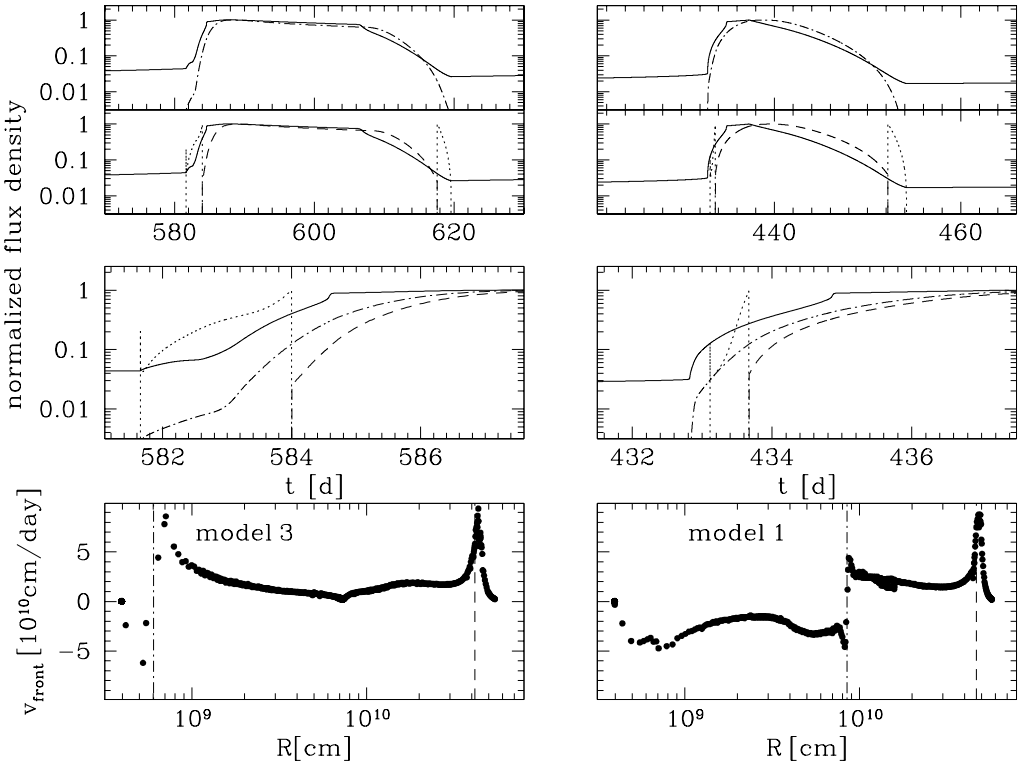

Fig. 3. The predicted normalized optical (solid line) and UV flux (dashed–dotted) as well as the normalized boundary layer emission, i.e. X-rays (dotted) and EUV (long dashed) for inside-out (left) and outside-in (right) outbursts. The intermediate panel shows a detailed view of the outburst rise, and the scale is the same for both models. The bottom panels show the heating front velocity corresponding to the rise of the outbursts. The ignition radius is marked by the vertical dashed–dotted line. The long dashed line on the right gives the position of the disc radius during quiescence. Having arrived at the outer edge, the plotted velocity gives no longer the speed of the heating front but that of the expansion of the disc.

(see Lin et al. 1985; Menou et al. 1999; Lasota 2001, for a detailed discussion). In contrast, an outside–in heating front starts in high surface density regions and has an easy way "downhill" sliding down along the gradients. They never die before fulfilling their task. Thus, for an outside–in front the accretion rate in the inner regions of the disc as well as the accretion rate onto the white dwarf increase much more rapidly than in the case of an inside–out heating front. As a consequence, the UV and EUV delay at the onset of the optical rise are significantly *shorter* than in the inside–out case. As the inward moving transition front is faster, the final stages of the rise are dominated by the inside–out part of the heating front and by the adjustment of the disc to the quasi stationary state. Hence, the delays measured closer to the maximum ($\Delta_{UV,0.5}$, $\Delta_{EUV,0.5}$) are nearly independent on the ignition radius.

The early rise of the accretion rate which is related to the X-ray flux is delayed relative to the optical by 0.3–0.45 days, i.e. the time it takes the heating front to reach the inner edge (see Figs. 3, 4).

4.1.3. Decline and quiescence

Clearly, during the late optical decline of every outburst our model predicts an increase of the X-ray emission when the mass accretion rate decreases below $10^{16}\,\mathrm{g\,s^{-1}}$ and the boundary layer is expected to become optically thin. Cooling fronts are slower than outside–in heating fronts but their velocity is comparable to that of inside–out heating fronts at small radii (see Menou et al. 1999, for a detailed study of the properties of transition fronts). Consequently, the predicted duration of the increased X-ray flux (in the following called the "X-ray on" state) is similar to that at the rise of an inside–out outburst (i.e. ∼2 days).

Finally we want to place emphasis on the predicted accretion rate during quiescence which is in the range of 10^{11}–$10^{13}\,\mathrm{g\,s^{-1}}$ for both outburst types. Notice, although the duration of the "X-ray on" state corresponds to the observed one, the calculated accretion rates during quiescence are several orders of magnitude lower than those deduced from observations. This will be discussed in more detail in Sect. 6.

4.2. Truncation of the inner disc

During the last decade it has been intensively discussed whether an optically thick accretion disc extends down to the white dwarf in quiescent dwarf novae. The main reason for this discussion was the serious discrepancy between calculated accretion rates and those deduced from X-ray observations. Disc truncation by evaporation (Meyer & Meyer-Hofmeister 1994) and/or by a magnetic field (Lasota et al. 1995; Hameury et al. 1997) could bring into agreement models and observations. Also the alleged difficulties of the DIM with the UV-delay

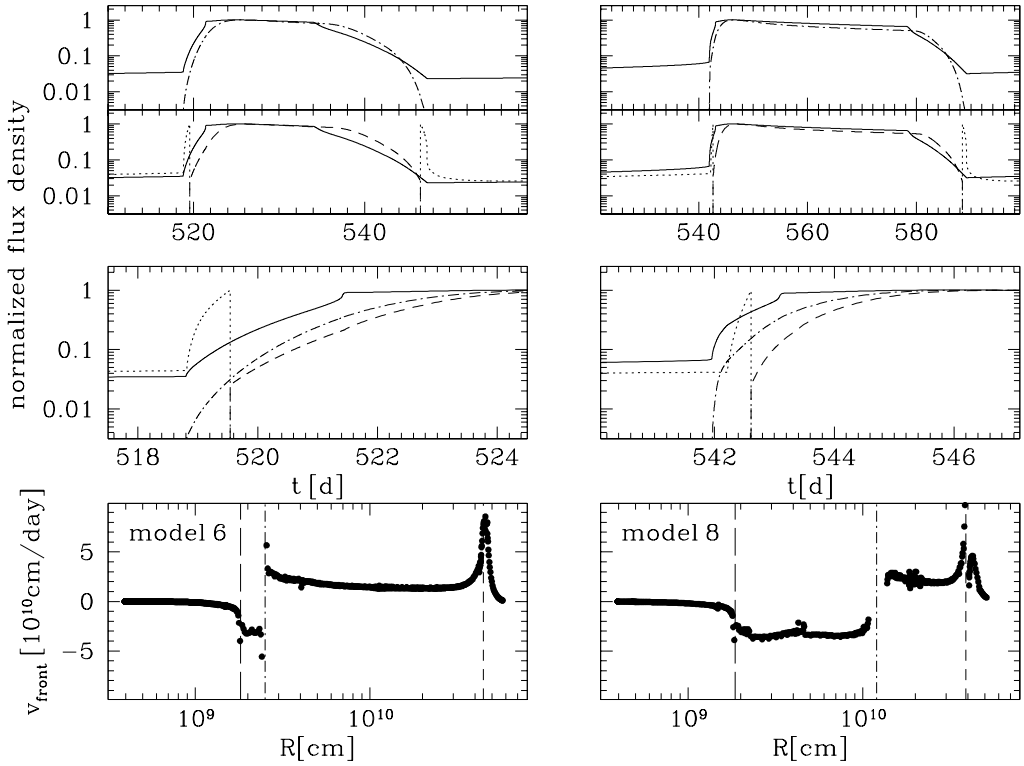

Fig. 4. Same as Fig. 3 but assuming the inner disc being truncated. Around $R = 2 \times 10^9$ cm the heating front reaches the inner edge of the disc indicated by the long dashed vertical line. Then the velocity decreases from the speed of the heating front to that of the inward expansion of the disc governed by Eq. (5). Note that the scale of the intermediate panel is the same as in Fig. 3.

motivated interest in truncated discs. King (1997) suggested that irradiation of the disc by the white dwarf can keep the inner disc in the hot ionized state leading to very low surface densities in this region[1] and Livio & Pringle (1992) analyzed the effects of a weakly magnetized white dwarf.

To discuss in detail each mechanism which has been proposed in the context of SS Cygni is beyond the scope of this paper. For our purpose it is sufficient just to assume the formation of an inner hole during quiescence. We assume here that the inner disc radius is given by the "magnetospheric" radius:

$$R_{\rm in} = R_{\rm M} = 9.8 \times 10^8 \, \dot{M}_{15}^{-2/7} {M_{\rm wd}}^{-1/7} \mu_{30}^{4/7} \ {\rm cm} \qquad (5)$$

where μ_{30} is the magnetic moment of the white dwarf in units of 10^{30} G cm^3 (Hameury & Lasota 2002).

Clearly, because the accretion flow is disrupted by the magnetic field, a boundary layer will not form when the disc is truncated. Instead, matter flows along the field lines, and its kinetic energy is released in a shock at the surface of the white dwarf. The spectral range of this emission depends on whether the flow is optically thin or not; for the sake of simplicity, we use the same condition as for the boundary layer case. This is an apparently crude approximation. Assuming, however, as an antithesis that the flow becomes optically thick precisely when the disc reaches the surface of the white dwarf would be equivalent to a small increase of $\dot{M}_{\rm cr}$ because the accretion rate onto the white dwarf exceeds 10^{16} g s^{-1} shortly before the disc reaches the white dwarf. Such a small increase of $\dot{M}_{\rm cr}$ would lead to somewhat higher values for the predicted duration of the "X-ray on" state and the early EUV delay ($\Delta_{\rm EUV,0}$) but not affect the conclusions of this paper.

Table 3 lists the delays we obtained for three different mass transfer rates and $\mu_{30} = 2$. Figure 4 shows the normalized flux densities and heating front velocities for two outbursts. The optical rise for inside–out outburst is faster than without truncation as the heating front is forced to start at $R_{\rm in} > R_{\rm wd}$, i.e. in a region with higher surface density (Fig. 4). Therefore, the delays $\Delta_{\rm UV,0}$ and $\Delta_{\rm EUV,0}$ are shorter than for inside–out outbursts without truncation. The predicted EUV delay of outside–in and inside–out outbursts becomes comparable whereas $\Delta_{\rm UV,0}$ remains significantly shorter for outside–in outbursts.

Truncation is also changing the situation for the early rise of the accretion rate which is correlated to the predicted hard X-ray flux. Considering the arrival of the heating front at the inner edge two effects have to be mentioned. First, the time it takes outside–in heating fronts to reach the inner edge decreases slightly because the heating front just has to reach $R_{\rm in} = R_{\rm M} > R_{\rm wd}$. Second, once the heating front reached $R_{\rm in}$ the disc starts filling the inner hole, i.e. $R_{\rm in}$ is decreasing. This process is rather slow compared to the heating front velocity (see Fig. 4). The increase of the mass accretion rate is therefore less sudden and the small spike seen in Fig. 3 disappears. The expected X-ray emission at the end of an outburst is also influenced by the presence of truncation. The initial velocity of cooling fronts is rather high but as it propagates inward it

[1] Disc irradiation does not however have the same consequences as plain disc truncation; for a detailed analysis of disc irradiation see Hameury et al. (1999); Stehle & King (1999); Schreiber & Gänsicke (2001).

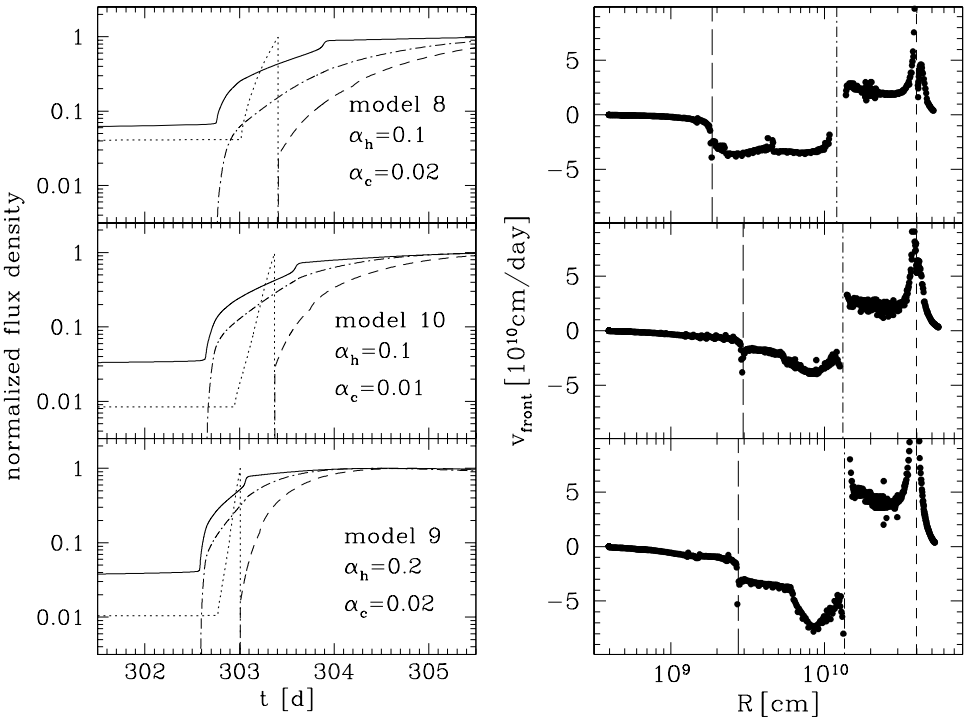

Fig. 5. The same as Figs. 3 and 4 but for different values of α. From top to bottom the plots correspond to models 8, 10, and 9 (see Table 3 for the predicted delays).

relaxes to an essentially lower speed which depends just on the location of the front (Menou et al. 1999). Consequently, if the inner disc is truncated, the cooling front is reaching earlier the inner edge which reduces the duration of the "X-ray on" state at the end of an outburst.

A final note on the effects of truncation concerns the accretion rate during quiescence: the postulation of an inner hole dramatically increases the predicted X-ray flux during quiescence (compare Figs. 3 and 4). Instead of 10^{11}–$10^{13}\,\mathrm{g\,s^{-1}}$ without truncation we obtain now $\dot{M}_{\rm acc} \sim 3$–$5 \times 10^{14}\,\mathrm{g\,s^{-1}}$. This increase of the expected X-ray emission during quiescence results from the fact that the DIM predicts accretion rates which increase with radius while the disc accumulates mass.

We want to stress that assuming evaporation (e.g. together with a radially extended optically thin boundary layer (Narayan & Popham 1993; Medvedev & Menou 2002)) instead of a weakly magnetic white dwarf would lead to almost identical results.

4.3. Changing α

The third part of Table 3 lists results obtained with different values of α. As long as this parameter is physically rather unconstrained, analyzing the DIM requires discussing different values of α. We calculated again light curves with $\mu_{30} = 2$ but increased (decreased) $\alpha_{\rm h}$ ($\alpha_{\rm c}$). As we choose a high mass transfer rate ($\dot{M}_{\rm tr} = 15 \times 10^{16}\,\mathrm{g\,s^{-1}}$) the outbursts are of the outside–in type.

Increasing $\alpha_{\rm h}$ (model 9, Fig. 5, bottom) or decreasing $\alpha_{\rm c}$ (model 10, Fig. 5, middle) leads to smaller accretion rates during quiescence. This is because the accretion rate on the lower branch of the S-curve corresponding to $\Sigma_{\rm min}$ decreases when the ratio $\alpha_{\rm h}/\alpha_{\rm c}$ becomes larger. Thus, in model 9 as well as model 10 the part of the disc being truncated during quiescence becomes larger (see Fig. 5).

Conversely, the accretion rate on the upper branch which corresponds to $\Sigma_{\rm max}$ is increasing with $\alpha_{\rm h}/\alpha_{\rm c}$. Thus, after the outside–in heating front passes the inner disc regions, the accretion rate there is higher for models 9 and 10 reducing the predicted UV-delay. In the case of model 9 the UV delay is additionally shortened as the higher value of $\alpha_{\rm h}$ leads to faster heating fronts (see Fig. 5).

Considering the EUV delay we find drastic changes only in the case of increased $\alpha_{\rm h}$ (compare model 8 and model 9). This shows that the EUV delay is mainly governed by the viscous time scale. Due to the increase of $\alpha_{\rm h}$ it takes the disc less time to reach high accretion rates.

4.4. Variations of the mass transfer rate

So far we presented light curves assuming the accretion disc has adjusted to the prevailing constant mass transfer rate and is going through the same outburst cycle all the time. Inspecting Fig. 1 indicates that for SS Cyg this is not the case: for example the first as well as the forth panel show extremely irregular outburst behaviour. In addition, no constant mass-transfer rate model can reproduce alternating outside-in and inside-out outbursts.

Considering the obvious irregularities in the light curve we should take into account mass transfer variations. Recently there has been a debate about the strength of possible mass transfer variations in dwarf novae. It has been shown that

Z Cam light curves can be explained assuming only small fluctuations (∼30%) of the mass transfer rate if additional heating of the outer edge is considered Buat-Ménard et al. (2001). On the other hand the dwarf nova system RX And has occasionally much stronger mass transfer variations and is blend of a Z Cam star and VY Scl star (Schreiber et al. 2002; Hameury & Lasota 2002). However, because the long term light curve of SS Cygni is in general rather "regular" we assume that variations of the mass transfer rate in SS Cyg do not exceed the strength necessary to explain Z Cam standstills[2] and use

$$\dot{M}_{\rm tr} = \dot{M}_{\rm tr,0}(1 + 0.15\sin(\pi\, t_{100})), \quad (6)$$

where t_{100} is the time in units of 100 days. This prescription for variations of the mass transfer rate is obviously arbitrary but, nevertheless, the numerical experiment might give us a hint about the nature of mass transfer variations in SS Cyg.

The disc reacts on the varying mass transfer rate with alternating long and short outbursts. This is not surprising as earlier calculations (e.g. King & Cannizzo 1998; Schreiber et al. 2000) have shown that the disc rather quickly adjusts itself to a given mass transfer rate. Our calculations confirm the result of Buat-Ménard et al. (2001) that small mass transfer variations can lead to alternating inside–out and outside–in outbursts. Moreover, the long term light curve contains long and short outbursts of both types. The resulting delays are given in Table 3 (model 11). Evidently, smooth, periodic and small variations of the mass transfer rate do not change anything as they do neither essentially affect the properties of the heating fronts nor influence the viscous time scale.

5. Comparison with earlier calculations

As the UV delay has been discussed intensively in the literature we should relate our results to previous calculations. After observational evidence for the existence of the UV delay established several papers stating that the predicted delay is too short appeared (e.g. Cannizzo & Kenyon 1987). The reasons for this and later similar assertions are discussed in detail in the excellent paper by Smak (1998).

In this paper Smak presented a model similar to the one specified in Sect. 3. Having calculated light curves for a set of parameters Smak (1998) concluded that the DIM predicts correct UV delays if one uses the correct boundary conditions and sufficiently large discs: the delay just depends on whether an outside–in (long delay) or an inside–out outburst (short delay) develops.

However, Smak (1998) did not consider heating of the disc due to the stream impact and tidal dissipation. Without these additional physical effects Smak was unable to obtain outside-in (type A – in his terminology) outbursts for a binary with SS Cyg parameters: the required high mass-transfer rates would correspond to steady accretion. Smak (1998) therefore used binary parameter different from those listed in Table 2, which were not directly applicable to SS Cyg; in fact his discs are too small for this system. In addition we note that Smak used another approximation for the emission of the boundary layer and the accretion disc during quiescence.

[2] In fact SS Cygni is expected to show the Z Cam phenomenon (Buat-Ménard et al. 2001).

Table 4. The predicted UV delay when using the same orbital parameter as Smak (1998). Models 1s and 2s are calculated using our model described in Sect. 3 whereas in models 3s and 4s we used Smak's treatment of the boundary layer emission, and neglected (as he does) additional heating of the outer disc and irradiation of the secondary.

Model	$\dot{M}_{\rm tr}$	$\Delta_{\rm UV,0}$	$\Delta_{\rm UV,0.5}$	$R_{\rm init}$	W
	$[10^{16}\,{\rm g\,s^{-1}}]$	[d]	[d]	$[10^{10}\,{\rm cm}]$	[d]
1s	8	0.9	0.6	0.075	22
2s	10	0.1	0.5	1.2	37
3s	15	1.1	1.2	0.078	9
4s	30	0.4	1.1	2.44	10

To compare our results with Smak's findings we again calculate outburst using the model described in Sect. 3 but assuming $M_{\rm wd} = 1\,M_\odot$, $M_{\rm sec} = 0.4\,M_\odot$, $P_{\rm orb} = 4.2\,{\rm hr}$, $< R_{\rm out} > = 4.2\times10^{10}\,{\rm cm}$ and $\dot{M}_{\rm tr} = 8, 10\times10^{16}\,{\rm g\,s^{-1}}$ (models 1s and 2s in Table 4 which correspond to models 13 and 14 of Smak 1998). We also performed simulations without including heating due to the stream disc impact and tidal dissipation, assuming that the boundary layer luminosity is thermalized over the surface of the white dwarf, i.e. $f_{\rm em} = 1$ in Eq. (2), and neglecting irradiation of the secondary (models 3s and 4s in Table 4). Apart from the different treatment of the lower branch of the S-curve models 3s and 4s are identical to Smak's simulations. Due to the absence of additional heating of the outer disc we require higher values for the mass transfer rate to produce large outbursts, i.e. $\dot{M}_{\rm tr} = 1.5\times10^{17}\,{\rm g\,s^{-1}}$ and $\dot{M}_{\rm tr} = 3.0\times10^{17}\,{\rm g\,s^{-1}}$. The resulting delays are listed in Table 4.

Figure 6 compares the contribution of disc, boundary layer, white dwarf, hot spot, and irradiated secondary for models s1 and s2. Emission from the disc dominates at UV as well as optical wavelengths. The irradiated secondary accounts for ∼10% of the visual emission. In contrast, using Smak's prescription (models 3s and 4s; Fig. 7) the boundary layer contributes significantly to the UV (middle panel in Fig. 7) and neglecting irradiation of the secondary reduces the predicted optical emission (top panel of Fig. 7). In addition, ignoring heating of the outer disc allows us to obtain outside–in outbursts which are triggered at essentially larger radii, i.e. $R_{\rm init} = 2.4\times10^{10}\,{\rm cm}$. Due to these changes the UV-delay becomes longer (see Table 4).

Considering outside–in and inside–out outbursts our previous findings are confirmed: the UV delay is *longer* for inside-out outbursts at the onset of the optical rise and comparable close to the maximum. We note that in Smak's calculations the instability is triggered at larger radii. In model 13 of Smak (1998) the heating front starts at $R_{\rm init} = 3.5\times10^{10}\,{\rm cm}$ whereas we do not obtain a comparable large ignition radius ($R_{\rm init}$ in Table 4). This is probably due to the different treatment of the lower branch of the S curve (Smak, private communication).

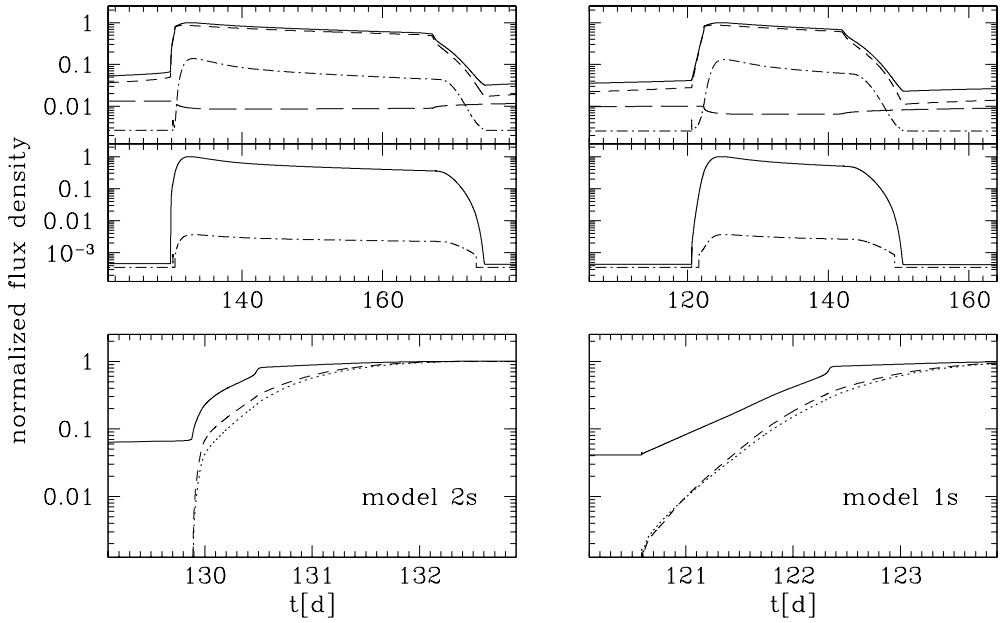

Fig. 6. Comparison of inside–out (right) and outside–in (left) outbursts calculated using the same parameter as Smak (1998). The top panel compares the contribution to the optical flux (solid line) from disc (short dashed), irradiated secondary (dashed–dotted), and bright spot (long dashed). For the UV flux only emission from the disc (second panel, solid line) is important. The boundary layer contribution (dashed dotted) is less than one percent. The bottom panel shows the rise of the outbursts for the optical flux (solid line) and the UV flux assuming Kurucz (dashed) and blackbody (dotted) spectra.

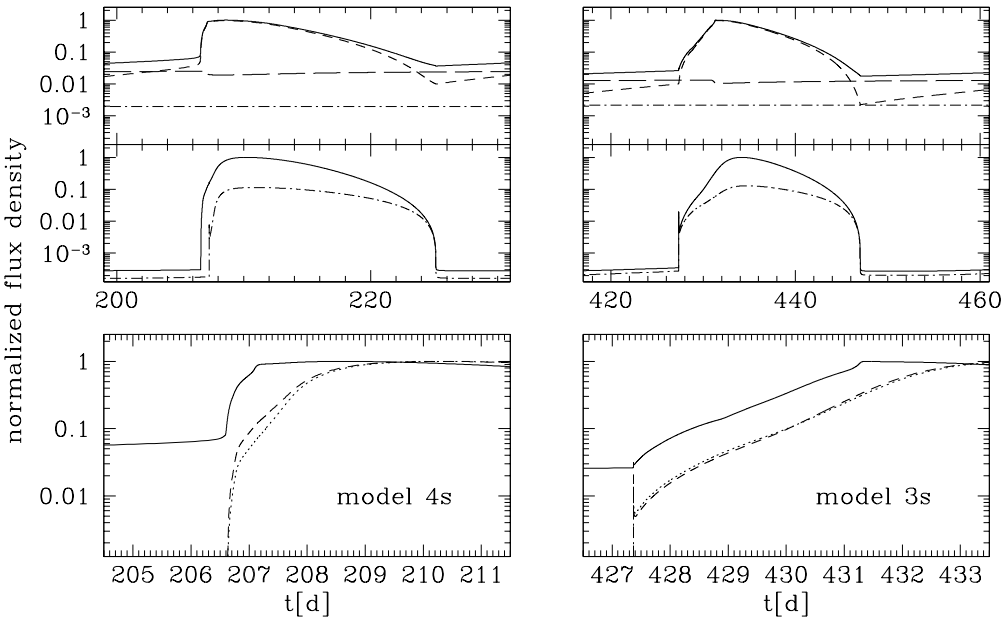

Fig. 7. The same as Fig. 6 but neglecting heating due to stream impact and tidal dissipation and using Smak's approximation for the emission from the boundary layer and the secondary (see text). Although the ignition radius is larger for the outside–in outburst ($R_{\rm init} = 2.4 \times 10^{10}$ cm) the UV delay (bottom panels) remains somewhat longer for outside–in outbursts (see also Table 4).

In Figs. 6 and 7 we also plotted the UV light curve calculated by summing blackbody spectra. In agreement with Smak's finding, the UV blackbody light curves are somewhat delayed (~0.01–0.1 d) to the Kurucz ones.

Hameury et al. (1999) calculated the EUV delay for SS Cyg parameters, assuming that EUV emission is directly proportional to the accretion rate onto the white dwarf when the disc reaches its surface, i.e. when a boundary layer forms. They also assume that truncation of the inner disc but due to evaporation instead of a magnetic field However, their inner disc radius in quiescence is comparable to the one used here and despite of the different assumptions, the EUV delay they obtain (1 day) is in good agreement with the value found here, showing that the detailed mechanism causing the disc truncation is of little importance.

Regarding the case study of Cannizzo (2001) we stress the same difference as to Smak's calculations: even for outside–in outbursts the heating front does not start close to the outer edge but at a distance of $\sim 1-2 \times 10^{10}$ cm from the white dwarf.

A final note concerns the EUV: both authors (Cannizzo 2001; Smak 1998) assume that the EUV delay is almost identical to the time it takes the heating front to reach the inner edge of the disc. Our model takes recent X-ray observations (see Sect. 2) into account which indicate that this is not true. Moreover, our calculations predict that the EUV delay close to maximum is governed by the time it takes the disc to enter into the quasi-stationary state whereas the delays at the beginning of the optical rise also depend on properties of the heating front and $\dot{M}_{\rm cr}$.

6. Discussion: Model versus observations

In this section we compare our results with the observations outlined in Sect. 2. It is *not* however the goal of this paper to try to reproduce the observations by using the whole parameter space. Instead, we analyzed systematic dependencies of the model on rather unconstrained parameter to see whether comparison with observations may help to guess their values.

6.1. X-rays

There has been only one SS Cyg outburst which was observed simultaneously in X-rays and EUV. The observed long delay (0.9 days) for the rise of the X-rays indicates that this outburst was of the outside–in type as our calculations predict no delay for inside–out outbursts. However, the X-ray delay predicted by the calculated outside–in outbursts is shorter than the observed one by a factor of ∼2–3.

The obtained durations of the "X-ray on state" during the optical rise (∼0.5 days) as well as at the end of the outburst (∼2 days) are in perfect agreement with the observed ones (see Wheatley 2000; Wheatley et al. 2003).

Comparing the observed X-ray flux during quiescence with the calculated mass accretion rate strongly suggests that the inner disc is truncated. Truncation leads to *higher* accretion rates during quiescence as accretion increases with radius while the disc accumulates mass.

Concerning the X-ray delay and the duration of the "X-ray on" state one should note that our results are obviously sensitive to $\dot{M}_{\rm cr}$.

6.2. The UV delay

Generally, the delay between the optical and the UV rise is comparable to the observed one (which has always been found to be of order of half a day, see above) for models 1–8, and 11 (see Tables 1 and 3). Although the delay is somewhat *longer* for inside–out outbursts, the agreement between observations and calculations is independent on whether the heating front starts close to the white dwarf or not. Thus, the UV delay is *not* a good indicator of the outburst–type.

The UV delay sensitively depends on α (see Sect. 4.3). We obtain good agreement with $\alpha_{\rm h} = 0.1$, and $\alpha_{\rm c} = 0.02$.

6.3. The EUV delay

6.3.1. Normal outbursts

At first we consider the so called normal outbursts (see Fig. 1 and Table 1). These outbursts are characterized by a fast optical rise and are therefore generally thought to be of the outside–in type. We find the calculated EUV delay at half the maximum optical flux ($\Delta_{\rm EUV,0.5}$) being nearly independent on the radius at which the heating front was triggered (Table 3) but in excellent agreement with the observed delay. Our model predicts a somewhat lower value at the onset of the optical rise ($\Delta_{\rm EUV,0}$) than it is observed except for inside–out outbursts without truncation. We note that $\Delta_{\rm EUV,0}$ sensitively depends on the assumed value of $\dot{M}_{\rm cr}$ and the optical flux in quiescence (the effective temperature of the secondary might be higher than 4000 K as suggested e.g. by Webb et al. 2002). Of course, it would be possible to perfectly match the observed $\Delta_{\rm EUV,0}$ also in the case of outside–in outbursts with truncation. To sum up, the model can reproduce the EUV delay measured for normal outbursts.

6.3.2. Anomalous outbursts

The standard α-model, even modified by truncation, various types of heating etc., cannot reproduce the observed light curve of anomalous outbursts. The model does never predict a rise time comparable to that of the outburst observed in 1999 (∼17 d; Fig. 1, bottom panel). The observed rise time of the anomalous outburst in 1993 (∼5 d; Fig. 1, second panel from top) can only be reproduced if we assume that the disc extends down to the surface of the white dwarf (i.e. no truncation) and if we additionally completely neglect both heating of the outer disc due to the stream impact and tidal dissipation. In this case, however, the calculated light curve does not have the observed flat top which is as bad as the prediction of a too short rise time. In addition, without truncation the model predicts several small outbursts between the larger ones which is not observed (Fig. 2), and also the predicted X-ray flux is far too small (see Sects. 4.1 and 4.2).

In view of this incapacity of the model, trying to find the corresponding delays appears totally pointless. However, attempting to find models with time lags close to those observed could be a useful diagnostic tool for future developments.

As mentioned, we have to distinguish between the 1993 (second panel Fig. 1) and the 1999 (bottom panel) event as their properties are very different. Considering the 1999 eruption we note that the long delay between the optical and the EUV measured at the onset of the optical rise of the anomalous outbursts (Table 1) is not reproduced even by rather long inside–out outbursts without truncation (i.e. model 3). Assuming the inner disc being truncated, the situation becomes even worse as $\Delta_{\rm EUV,0}$ gets shorter. In addition, our simulations disagree with the observed drastic decrease of the EUV delay with increasing optical flux (Table 1, Mauche et al. 2001). It is especially the observed slow optical rise and not the shape of the EUV light curve which differs from the predictions. Inspecting Fig. 1 we find the outburst being a part of strong deviations from regular outburst behaviour: there was no quiescence at all between this

outburst and the previous one. It is then not at all surprising that the model cannot reproduce the EUV delay of this particular outburst. Such a disruption of the light curve can only be due to a change in one of the parameters assumed here to be constant. The mass transfer rate could for example have changed drastically, or the Shakura-Sunyaev parameterization of the viscosity could have been affected by e.g. a magnetic flare in the disc; there are many possibilities, and it is far beyond the scope of this paper to investigate them in detail.

For the 1993 outburst we note that our calculations hardly agree with the long delay at the onset of the optical rise. Especially if the inner disc is truncated (which is strongly suggested by the quiescence X-ray flux) the obtained value for $\Delta_{\rm EUV,0}$ is smaller than observed even for inside–out outbursts whereas for the predicted time lags closer to the maximum the opposite holds. Of course, $\Delta_{\rm EUV,0}$ still depends on the approximation of the boundary layer (e.g. $\dot{M}_{\rm cr}$) and the optical emission during quiescence (secondary). We certainly would be able to construct a delay of three days but in any case the model predicts a significant delay closer to the maximum. This prediction of the model is firm as the EUV emission reaches maximum when the disc has adjusted to the quasi-stationary state whereas the optical flux is already close to maximum when the heating front has gone through the outer disc region. However, the obtained disagreement could be related to the three low-amplitude anomalous outbursts preceding by ∼20 days the anomalous 1993 outburst.

6.4. The EUV spectrum

Mauche et al. (1995) present EUVE observations of SS Cyg during the outburst in 1993 between August 17.1 and 23.6. They find a remarkable correlation between the hard (72–90 Å) and soft (90–130 Å) count rate. Even during the rise of the outburst the ratio of the two remains constant. On the other hand, more recent observations of another outburst show that the hardness ratio may change by a factor of ∼3 (Wheatley et al. 2003). Although our assumptions for the boundary layer are quite rough, we calculate the hardness ratio predicted by the model to get a hint of the uncertainty linked to the black body approximation.

Assuming $N_{\rm H} = 4.4 \times 10^{19}\,{\rm cm}^{-2}$, making use of the cross-sections as a function of wavelength according to Morrison & McCammon (1983) by interpolating their Table 2, we simulated the evolution of the EUV spectrum during an outburst. Figure 8 shows the normalized integrated flux (70–130 Å), monochromatic 100 Å flux, and the hardness ratio defined as H = flux(70–90 Å)/flux(90–130 Å) for model 1. We find H varying between 2 and 4 which appears to be in reasonable agreement with the count rate hardness ratio given by Wheatley (2000) and Mauche et al. (1995).

6.5. Bandpass fluxes

So far we have presented monochromatic model light curves and compared the obtained delays with the observed time lags. Here we verify that our monochromatic approach is reasonable.

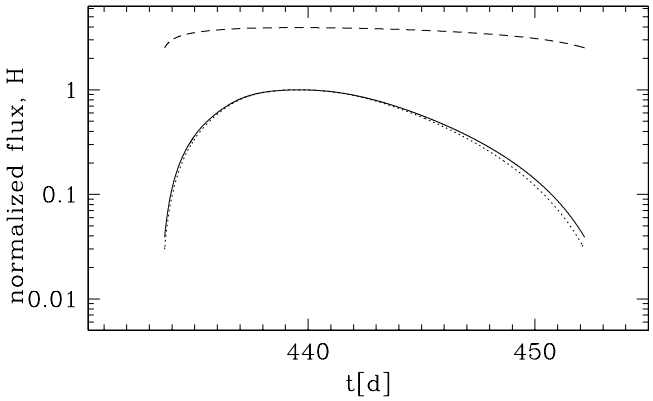

Fig. 8. Normalized monochromatic flux at 100 Å (solid line), integrated EUV flux (70–130 Å; dotted line), and the EUV hardness ratio (dashed line).

Figure 8 confirms that the EUV light curve is well represented by the 100 Å emission. The suitability of the monochromatic light curves is further established in Fig. 9 where we present both the predicted normalized flux densities at 5500 Å and 100 Å (top panel) and the corresponding integrated optical and EUV fluxes (bottom panel). Apparently, the light curves and especially the predicted delays are very similar. The only difference worth mentioning concerns the optical emission: compared to the monochromatic light curves the relative contribution of the hot spot emission increases, which leads to relatively brighter quiescence. Concerning the delays we conclude that the monochromatic light curves can be considered as representative for the emission in the corresponding bandpasses.

6.6. Absolute values

Discussing the absolute emission in addition to the normalized monochromatic light curves requires to assume a distance for SS Cygni. Recently Harrison et al. (1999) measured a parallax using the HST Fine Guiding Sensor (FGS) and derived a distance of $d = 166 \pm 12$ pc which is essentially larger than previously thought. We want to stress here that, according to the model, the distance of SS Cygni cannot be 166 pc. In all the calculations performed for this paper the maximum accretion rate hardly reaches $\dot{M}_{\rm acc} = 10^{18}\,{\rm g\,s}^{-1}$ which is far too low to explain the observed visual brightness of the system if its distance indeed was 166 pc. As shown by Schreiber & Gänsicke (2002), at such a large distance SS Cyg would not be dwarf nova: the accretion rate required to reproduce the observed visual brightness would certainly lead to stationary accretion[3].

Instead of the large HST/FGS distance we therefore assume a more traditional and, according to the model, more realistic value for the distance of SS Cygni, i.e. $d \sim 100$ pc (e.g. Warner 1987; Bailey 1981; Kiplinger 1979). The order of the maximum monochromatic emission of the light curves presented in Figs. 3–5 is the following: the lowest flux density is expected

[3] It is worth noting that problems with the small HST/FGS–parallax have been mentioned by North et al. (2002) too. The space velocity they derive assuming $d = 166$ pc is essentially larger than theoretically expected.

at the optical wavelength ($\sim 1.5 \times 10^{-14}$ erg cm^{-2} s^{-1} Å^{-1}) followed by the UV ($\sim 3.3 \times 10^{-13}$ erg cm^{-2} s^{-1} Å^{-1}) and the EUV ($\sim 2-12 \times 10^{-11}$ erg cm^{-2} s^{-1} Å^{-1}). These values are calculated assuming an inclination of $i = 37^{\circ}$. The EUV emission depends strongly on the assumed hydrogen column density. The range of values given above is determined assuming $N_{\rm H}$ being between 10×10^{19} cm^{-2} and 4.4×10^{19} cm^{-2}. In Fig. 9 we also give absolute band integrated optical and EUV (70–130 Å) fluxes.

Comparison with Fig. 1 shows that the obtained maximum visual magnitude agrees well with the observations. Furthermore, our calculations predict that the maximum UV flux density exceeds the optical one by a factor ~30 which is also in very good agreement with the observations (Cannizzo et al. 1986). The calculated absolute EUV emission is certainly the most uncertain one as it does not only sensitively depend on $N_{\rm H}$ but also on uncertainties related to the temperature and fractional emitting region of the boundary layer. Indeed, taking these difficulties into account, it has been shown by Wheatley et al. (2003) that the range of blackbody luminosities for which the observed EUV spectrum can be fitted is uncertain by more than one magnitude. Hence, trying to constrain the model using absolute EUV fluxes seems not very promising. Nevertheless, for completeness we note rough agreement between our calculations and the observations (see e.g. Mauche et al. 1995; Mauche 2002) for large hydrogen column densities, i.e. $N_{\rm H} \gtrsim 10^{20}$ cm^{-2}.

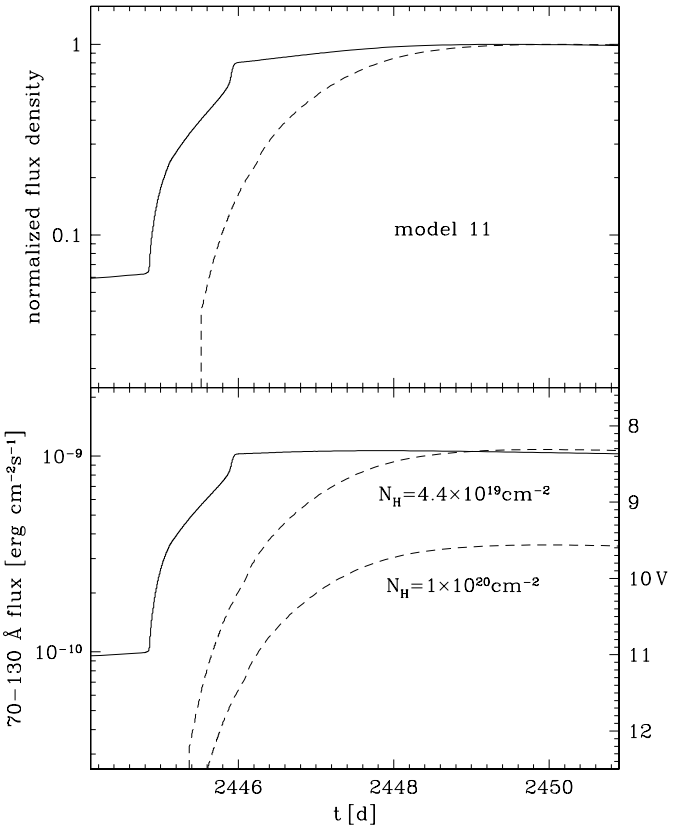

Fig. 9. Light curves of the long outside–in outburst we obtain assuming small variations of the mass transfer rate (model 11). Top panel: normalized flux density at 5500 Å (solid line) and 100 Å (dashed line). Bottom panel: visual magnitude and integrated 70–130 Å flux assuming $d = 100$ pc.

6.7. The long term light curve

Although the main goal of this paper is to analyze the time lags in SS Cyg, the predicted long term light curve is an essential feature which must agree with observations for the parameters that best explain the delays. The outburst cycles depend on the details of modeling. The parameter we chose lead to three different cycles (Fig. 2). With the disc extending down to the white dwarf, we get several small inside–out outburst between the major eruptions that are not observed. Truncation of the inner disc suppresses these small outbursts and the light curve consists only of large outbursts. If in addition small fluctuations of the mass transfer rate are included, it is possible to obtain alternating short and long outbursts of both types. Obviously, the latter hypothesis is favoured. Getting irregularities comparable to those seen in the observed light curve (see e.g. second and last panel from the top in Fig. 1) requires a major revision of the model.

7. Conclusion

We present a physically realistic model for dwarf novae consisting of the disc instability model (Hameury et al. 1998) and simple but reasonable assumptions for the emission of the boundary layer. We calculated dwarf nova light curves using parameters appropriate for SS Cygni to investigate time lags observed between the rise at different wavelengths. The results from this study are:

1. The UV delay strongly depends on where one measures it. Close to maximum it is nearly independent of where the heating front started or whether the inner disc is truncated. The UV delay at the beginning of the optical rise is significantly *longer* when the heating front is triggered close to the white dwarf.
   The UV delay is not at all a good indicator for the outburst type and it is sensitive to the value of α. We find reasonable agreement with observations for $\alpha_{\rm c} = 0.02$ and $\alpha_{\rm h} = 0.1$.
2. The agreement between observed and predicted EUV delay is satisfying for normal outbursts whereas the model fails to reproduce anomalous outbursts.
3. The increased X-ray flux observed between the optical and the EUV rise is a natural outcome of outside–in outbursts. At the end of every outburst the model predicts a rise of the X-rays comparable to the observed one. X-ray observations during quiescence strongly support the idea of truncation of the inner disc.

Acknowledgements. We are grateful to Chris Mauche for very helpful comments and advice. This research has made use of the AFOEV database, operated at CDS, France. MRS acknowledges funding by an individual Marie-Curie fellowship. This work has benefited from developments made by V. Buat-Ménard during his Ph.D. Thesis. JPL thanks Chris Mauche for enlightening discussions about various delays.

References

Bailey, J. 1981, MNRAS, 197, 31
Balbus, S. A. 2002, in The Physics of Cataclysmic Variables and Related Objects, ASP Conf. Ser., 261, 356
Balbus, S. A., & Hawley, J. F. 1998, Rev. Mod. Phys., 70, 1
Buat-Ménard, V., Hameury, J.-M., & Lasota, J.-P. 2001, A&A, 366, 612
Buat-Ménard, V., Hameury, J.-M., & Lasota, J.-P. 2001, A&A, 369, 925
Cannizzo, J. K. 2001, ApJ, 556, 847
Cannizzo, J. K., & Kenyon, S. J. 1987, ApJ, 320, 319
Cannizzo, J. K., & Mattei, J. A. 1992, ApJ, 401, 642
Cannizzo, J. K., Wheeler, J. C., & Polidan, R. S. 1986, ApJ, 301, 634
Done, C., & Osborne, J. P. 1997, MNRAS, 288, 649
Hameury, J., Menou, K., Dubus, G., Lasota, J., & Hure, J. 1998, MNRAS, 298, 1048
Hameury, J.-M., & Lasota, J.-P. 2002, A&A, 394, 231
Hameury, J. M., Lasota, J. P., & Dubus, G. 1999, MNRAS, 303, 39
Hameury, J. M., Lasota, J. P., & Huré, J. M. 1997, MNRAS, 287, 937
Harrison, T. E., McNamara, B. J., Szkody, P., et al. 1999, ApJ, 515, L93
Idan, I., Lasota, J.-P., Hameury, J.-M., & Shaviv, G. 1999, Phys. Rep., 311, 213
King, A. R. 1997, MNRAS, 288, L16
King, A. R., & Cannizzo, J. K. 1998, ApJ, 499, 348
Kiplinger, A. L. 1979, ApJ, 234, 997
Kurucz, R. L. 1979, ApJS, 40, 1
Kurucz, R. L. 1993, VizieR Online Data Catalog, 6039, 0
Lasota, J.-P. 2001, New Astron. Rev., 45, 449
Lasota, J. P., Hameury, J. M., & Hure, J. M. 1995, A&A, 302, L29
Lin, D. N. C., Faulkner, J., & Papaloizou, J. 1985, MNRAS, 212, 105
Livio, M., & Pringle, J. E. 1992, MNRAS, 259, P23
Mauche, C. W. 2002, in Continuing the Challenge of EUV Astronomy: Current Analysis and Prospects for the Future, ASP Conf. Ser., 264, 75
Mauche, C. W., Mattei, J. A., & Bateson, F. M. 2001, in Evolution of Binary and Multiple Star Systems, ASP Conf. Ser., 229, 367
Mauche, C. W., Raymond, J. C., & Mattei, J. A. 1995, ApJ, 446, 842
Medvedev, M. V., & Menou, K. 2002, ApJ, 565, L39
Menou, K., Hameury, J., & Stehle, R. 1999, MNRAS, 305, 79
Meyer, F., & Meyer-Hofmeister, E. 1994, A&A, 288, 175
Morrison, R., & McCammon, D. 1983, ApJ, 270, 119
Narayan, R., & Popham, R. 1993, Nature, 362, 820
North, R. C., Marsh, T. R., Kolb, U., Dhillon, V. S., & Moran, C. K. J. 2002, MNRAS, 337, 1215
Paczynski, B. 1977, ApJ, 216, 822
Patterson, J., & Raymond, J. C. 1985a, ApJ, 292, 550
Patterson, J., & Raymond, J. C. 1985b, ApJ, 292, 535
Ponman, T. J., Belloni, T., Duck, S. R., et al. 1995, MNRAS, 276, 495
Pringle, J. E., & Savonije, G. J. 1979, MNRAS, 187, 777
Schreiber, M. R., & Gänsicke, B. T. 2002, A&A, 382, 124
Schreiber, M. R., Gänsicke, B. T., & Mattei, J. A. 2002, A&A, 384, L6
Schreiber, M. R., & Gänsicke, B. T. 2001, A&A, 375, 937
Schreiber, M. R., Gänsicke, B. T., & Hessman, F. V. 2000, A&A, 358, 221
Sion, E. M. 1999, PASP, 111, 532
Smak, J. 1998, Acta Astron., 48, 677
Stehle, R., & King, A. R. 1999, MNRAS, 304, 698
Tylenda, R. 1981, Acta Astron., 31, 267
Vrielmann, S., Hessman, F. V., & Horne, K. 2002, MNRAS, 332, 176
Warner, B. 1987, MNRAS, 227, 23
Warner, B. 1995, Cataclysmic Variable Stars (Cambridge: Cambridge University Press)
Webb, N. A., Naylor, T., & Jeffries, R. D. 2002, ApJ, 568
Wheatley, P. 2000, in Rossi2000: Astrophysics with the Rossi X-ray Timing Explorer. March 22–24, 2000 at NASA's Goddard Space Flight Center, Greenbelt, MD USA, p. E83
Wheatley, P. J., Mauche, C. W., & Mattei, J. 2003, MNRAS, in press
Yoshida, K., Inoue, H., & Osaki, Y. 1992, PASJ, 44, 537